ANALYTICAL SCIENCES MARCH 2009, VOL. 25

2009 © The Japan Society for Analytical Chemistry

Detailed Investigation on the Possibility of Nanoparticles of Various Metal Elements for Surface-Assisted Laser Desorption/Ionization Mass Spectrometry

Tetsu YONEZAWA,*† Hideya KAWASAKI, Akira TARUI,** Takehiro WATANABE,** Ryuichi ARAKAWA,** Toshihiro SHIMADA,* and Fumitaka MAFUNÉ*****

**Department of Chemistry, School of Science, The University of Tokyo, Hongo, Bunkyo, Tokyo 113–0033, Japan*
***Department of Applied Chemistry, Faculty of Engineering, Kansai University, 3-3-35 Yamate-cho, Suita, Osaka 564–8680, Japan*
****Department of Basic Science, Graduate School of Arts and Sciences, The University of Tokyo, Komaba, Meguro, Tokyo 153–8902, Japan*

In this paper, we describe systematic detailed considerations of the feasibility of using various metal nanoparticles for organic-matrix-free surface-assisted laser desorption/ionization mass spectrometry (SALDI-MS). In order to avoid the influence of organic molecules on the nanoparticles, stabilizer-free bare nanoparticles of Ag, Au, Cu and Pt were prepared by laser ablation. Although all metal nanoparticles absorbed N_2 laser light (337 nm) energy, the performance of desorption/ionization of a representative peptide, angiotensin I, strongly depended on the metal element. Citrate buffer was used as a proton source; it reduced the amount of alkali cation adducts present. Then, protonated molecules of analytes predominated in the mass spectra when Au and Pt nanoparticles were used. Pt nanoparticles showed the highest performance in SALDI-MS, owing to their smaller heat conductivity and higher melting temperature. The selective desorption of a cationic surfactant with longer alkyl chains and a peptide with methionine was also observed.

(Received October 22, 2008; Accepted December 25, 2008; Published March 10, 2009)

Introduction

Metal particles with nanometer-scale dimensions are of great interest owing to their unique and interesting properties.[1-6] The size-[7] and shape-dependent[8,9] physical, chemical and optoelectronic properties of metal nanoparticles have important applications in catalysis[4,10] and biosensing,[11,12] recording media[13] and photoscience.[14] For example, recently, gold and silver nanoparticles have been used in various analytical techniques, such as biological optical imaging,[15] bio(chemical) sensing,[11,12,16] and surface-enhanced Raman scattering (SERS),[17–19] according to their unique plasmon absorption in the visible light region. Nanoparticles of platinum-group metals have been widely applied as effective catalysts in various organic reactions.[4,20-22] Size-controlled gold nanoparticles have also been applied as oxidation catalysts; their activity is strongly affected by their size.[23-25]

Matrix-assisted laser desorption/ionization mass spectroscopy (MALDI-MS) has become a powerful tool for analyzing organic molecules with a relatively high molecular weight, such as biomolecules and synthetic polymers.[26-30] Inorganic clusters can also be examined by MALDI-MS.[31] In MALDI-MS, analyte compounds are embedded in a surplus of matrix, consisting of small organic molecules, and co-desorbed upon laser excitation. The organic matrixes have high resonant absorption at the laser wavelength. Although MALDI-MS has been successfully used for the analysis of biomolecules and synthetic polymers, it has not been used extensively in low-molecular-weight compounds (m/z <500 Da), owing to the relatively high intensity of background signals from organic matrixes, which usually have similar molecular weights.

More recently, nanomaterials[32-46] such as carbon nanotubes (CNT),[33] porous silicon,[34] silylated porous silicones,[35,36] titania sol-gel thin film,[37,38] silicon nanoparticles[39] and gold nanoparticles[40-44] have received much attention for use in surface-assisted laser desoption/ionization mass spectrometry (SALDI-MS), which utilizes these inorganic matrixes, because of their high surface areas, simple sample-preparation techniques, and flexibility of sample deposition under different conditions. Early in 1988, Tanaka *et al.* used for the first time 30-nm-diameter cobalt nanoparticles suspended in glycerol to analyze lysozyme and synthetic polymers.[27] Graphite powder in glycerol is also used for SALDI-MS[45,46] and mass imaging.[47]

McLean *et al.* have recently demonstrated that size-selected Au nanoparticles (AuNPs) with 2 – 10 nm diameters can be used in SALDI-MS under dry surface conditions for the detection of peptides, such as substance P and phosphopeptides.[43] In addition, it has been suggested that AuNP matrixes afford the preferential ionization of peptides. On the other hand, recently, our group has introduced the use of special-structured platinum nanomaterials to ionize various peptides and proteins including cytochrome *c* (*ca.* 12 kDa).[32] Platinum has a higher melting temperature than gold, and is well-crystallized even in nanodimensions. However,

† To whom correspondence should be addressed.
E-mail: tetsu@chem.s.u-tokyo.ac.jp

no systematic consideration of the ability of metal nanoparticles for SALDI-MS has been reported so far.

In this work, we investigated the mass application of metal nanoparticles (*i.e.*, Au, Pt, Ag and Cu) as SALDI matrixes for peptides, surfactants and synthetic polymers, to examine the effect of the metallic species of nanoparticles. We have demonstrated for the first time that the performance of what in SALDI-MS was largely dependent on the species of metal nanoparticles: Pt nanoparticles (PtNPs) were superior to other nanoparticles (AuNPs and AgNPs). This difference is discussed based on a laser-induced temperature increase in these metal nanoparticles. In addition, it was found that metal nanoparticles without protective agents developed in this study have great advantage on the SALDI-MS for peptide analysis.

Experimental

Reagents and chemicals

Water was purified using a Milli-Q system (>18 MΩ cm). Angiotensin I and substance P were from Wako Pure Chemical Industries Ltd. (Osaka, Japan) and used as received. Metal plates for laser ablation were purchased from local suppliers. Poly(ethylene glycol)s (PEGs, average molecular weight, M_W = 0.4, 1, 2, and 3 K for PEG400, PEG1000, PEG2000, and PEG3000, respectively) were obtained from Wako Pure Chemical (Japan). Poly(methyl methacrylate) (PMMA) (M_W = 1890 Da, M_w/M_n: 1.10) was obtained from Polymer Laboratories. α-Cyano-4-hydroxycinnamic acid (CHCA) and 2,5-dihydoxybenzonic acid (DHB) was purchased from Sigma-Aldrich (Milwaukee, WI). Metal plates were purchased from Nilaco (Tokyo, Japan). All the other chemicals used were obtained from Nacalai Tesque Co. (Tokyo, Japan).

Preparation of metal nanoparticles

Nanoparticles of gold, platinum, and silver were prepared by laser ablation in aqueous media.[48,49] Various metal nanoparticles can be obtained by this method. The preparation process is very simple. Clean ingots of the metals were put into water in a PTFE or glass beaker. The output of a second-harmonic (532 nm) Nd:YAG laser (Quanta Lay GCR-170 or Thales Laser SAGA PRO 220-10 FHG) operating at 10 Hz was focused on the surface of the metal plates at the bottom of the beaker. The laser beam irradiation time was within 10 – 20 min. The spot sizes on the surface of the metal plates ranged from 1 to 3 mm. No stabilizing molecules were added to the sample dispersion. Some flocculation was observed when the dispersion was concentrated, because in this study no stabilizing reagent was used.

A copper nanoparticle (CuNP) dispersion also prepared by laser ablation was supplied from Fukuda Metal Foil and Powder Manufacturing Co. (Kyoto, Japan). No stabilizing reagent was added to a dispersion.

Citrate stabilized gold nanoparticles were prepared using a protocol proposed by Frens *et al.*[50] PVP (poly(*N*-vinyl-pyrrolidone))-stabilized gold and platinum nanoparticles were prepared by the alcohol reduction of $HAuCl_4$ and H_2PtCl_6 proposed by Yonezawa.[20] PVP is a frequently used water-soluble polymer for metal nanoparticle preparation.

Apparatus

SALDI and MALDI mass spectra were acquired in both the positive reflectron mode and the linear mode using an AXIMA-CFR time-of-flight mass spectrometer (Shimadzu/Kratos, Manchester, UK) with a pulsed nitrogen laser (337 nm). Analyte ions were accelerated at 20 kV under delayed extraction conditions.

Various nanoparticles (*i.e.*, AgNPs, AuNPs, CuNPs, and PtNPs) were used as the matrix for SALDI-MS. A two-layer sample preparation method was employed:[37] The first step was spotting the NPs solution (2×10^{-6} cm^3) on a stainless-steel plate, followed by drying. The second step was depositing the sample solution (5×10^{-7} cm^3) on the plate. In some cases, centrifugation was performed to concentrate the nanoparticle dispersion. For peptide samples, the sample aqueous solution was mixed with a citrate aqueous solution (diammonium citrate (200 mmol dm^{-3})/citric acid (200 mmol dm^{-3}) 5:1.1 (v/v); pH = 4.5) to a final concentration of 10×10^{-6} mol dm^{-3} prior to MALDI-MS. For cationic surfactants with four types of alkyltrimetylammonium bromide (C16TAB, C14TAB, C12TAB, and C10TAB; see Supporting Information), equal concentrations (1 mM) were prepared. AuNPs and PtNPs were dispersed in each surfactant aqueous solution and separated from the solution by centrifugation to remove any excess surfactants. The cationic surfactants trapped by the isolated particles were characterized by SALDI-MS with AuNPs and PtNPs after simple washing with water.

Transmission electron microscopy (TEM) was carried out with a Hitachi HF-2000 field-emission-type TEM (200 kV).

UV-Vis absorption spectra of NP-supported quartz plates in a dried state were obtained at 25˚C using a Jasco Ubest-670 UV/Vis spectrometer.

Results and Discussion

Preparation of nanoparticles

We used in this study a laser ablation process to obtain metal nanoparticles. Among many preparative procedures of metal nanoparticles, the laser ablation process is the most clean wet process, because the particles are obtained from pure metal ingots or flakes without any additives, such as reducing reagents and stabilizing materials.[48,49] Even counter ions or ligand molecules of metal sauces do not remain in the nanoparticle dispersion by using this method. The flocculation of NPs was not observed for at least 7 days at the prepared concentration.[48,49] Sometimes, the NP dispersion should be concentrated for SALDI-MS application. In such cases, flocculation of NPs was sometimes observed. This preparation process is most suitable for SALDI-MS inorganic matrixes, because naked nanoparticles should be very important for SALDI-MS application in order to avoid any obstacle peaks from organic compounds that are used as stabilizing reagents.

UV-Vis spectra and TEM images

Figure 1(a) shows the absorption spectra of dried AgNPs, AuNPs, CuNPs, and PtNPs deposited on a quartz plate. Unfortunately, the amounts of particles are not unique in these spectra. The absorption spectra of these NPs show a broad band from the visible region into the ultraviolet region, and characteristic surface plasmon resonance (SPR) bands appear at 420, 520, and 620 nm for AgNPs, AuNPs, and CuNPs, respectively. PtNPs are black, and showed no such specific absorption peak in this region, but do show a relatively high absorbance in the UV region. The absorbance of these metal nanoparticles at a wavelength of 337 nm suggests that these NPs could be used as an assisting material in UV (337 nm nitrogen laser)-SALDI-MS.

The representative TEM images demonstrated that these NPs have diameters of about 2 – 30 nm. Ag (~10 – 30 nm) and Cu (~10 – 20 nm) nanoparticles showed wider size distributions

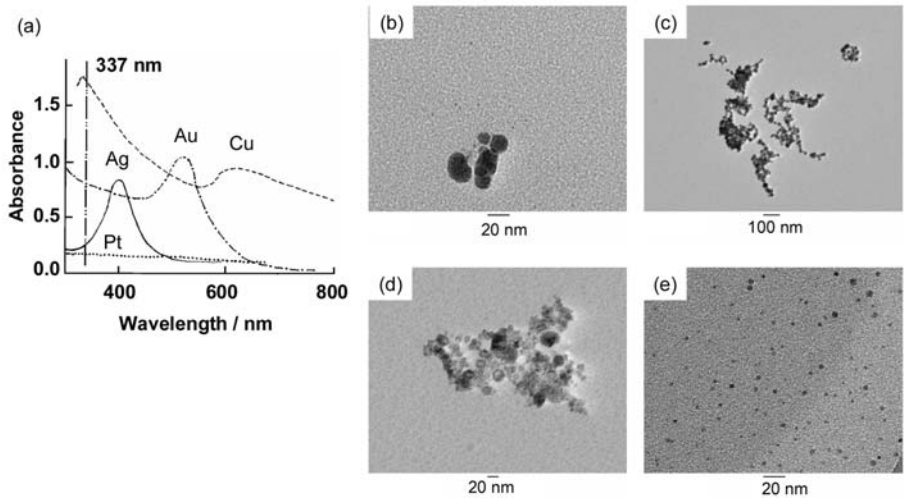

Fig. 1 (a) UV-Vis spectra and (b – e) representative transmission electron microscopy images of metal nanoparticles used for SALDI-MS plates: (b) Ag, (c) Au, (d) Cu, and (e) Pt. Ag nanoparticles are relatively large and Pt ones are smaller and unique.

Table 1 Diffusion lengths of the nanoparticle material metals

Metal	Density[63]/ 10^3 kg m^{-3}	Heat capacity[a63]/ J kg^{-1} K^{-1}	Heat conductivity[63]/ W m^{-1} K^{-1}	Diffusion length/nm[b]
Ag	10.5	235	429	144 – 277
Au	19.3	129	317	124 – 236
Cu	8.96	384	401	118 – 226
Pt	21.5	133	71.6	55 – 105

a. at 25˚C.
b. Calculated with Eq. (1). τ = 3 – 11 ns.

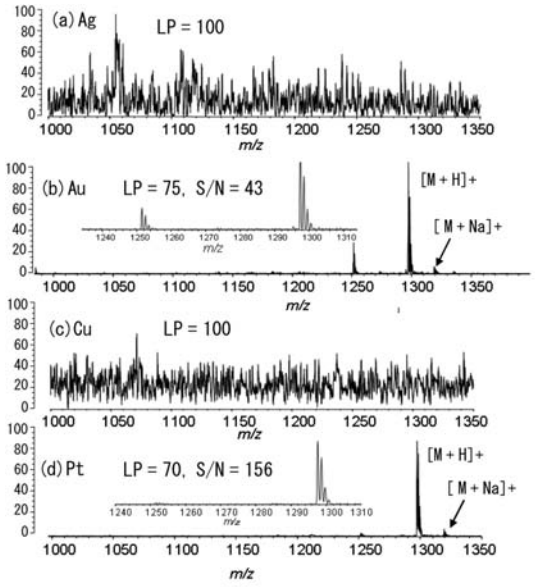

Fig. 2 SALDI-MS spectra of angiotensin I (500 fmol) obtained using (a) Ag, (b) Au, (c) Cu, and (d) Pt nanoparticles as SALDI matrixes. The irradiated laser power (LP) is shown. Ag and Cu nanoparticles could not ionize angiotensin I even at higher LP (LP = 100).

than Au (~20 nm) and Pt, as can be seen in the images. In the TEM images, the particles show aggregated structures, except in the case of platinum nanoparticles. These particles were produced in water, and the nanoparticles may form aggregations during the evaporation of water on the carbon-coated copper grids. Pt nanoparticles are smaller (~2 – 5 nm) than the others. These particles were smaller than Tanaka's cobalt nanoparticles (~30 nm),[27] and the particle size was much smaller than the heat diffusion length during the laser pulse duration, as discussed below (Table 1). Therefore, all of these particles should have enough ability to ionize organic molecules by laser irradiation heating.

SALDI-MS of angiotensin I

Figure 2 shows the mass spectra of angiotensin I obtained from the AuNPs, PtNPs, CuNPs, and AgNPs as SALDI matrixes. The stainless-steel sample plate, itself, without organic matrixes or metal nanoparticles shows poor ionization/desorption.[32,51] Angiotensin I is a typical peptide molecule for mass spectrometry analyses, and is often used as the material for the first screening of the SALDI ability for peptides. The insets in the figure show expanded views of the molecular ion region. Using AuNPs and PtNPs, we have successfully ionized angiotensin I in the proton adduct forms of $[M+H]^+$ (m/z = 1298 Da: Au, 130 mV; Pt, 58 mV) in the MS profile. We do not know, unfortunately, the actual value of a laser fluence in the instrument of SALDI-MS (Axima CFR, Shimadzu-Kratos) used in this study, although we know the relative values, denoted by the laser power, "LP". The laser power (LP) values used here were LP75 and LP70, respectively, and, furthermore, the signal/noise ratios of these spectra were high (S/N = 43 and 156, respectively). Also, the isotope peaks of angiotensin I were resolved in the case of AuNPs and PtNPs. A weak signal corresponding to the Na adduct form of $[M+Na]^+$ (m/z = 1320 Da: Au, 20 mV; Pt, 6 mV) appears to be adjacent to the $[M+H]^+$ peak for angiotensin I. In addition, a peak from the fragmentation of angiotensin I appears at m/z = 1250 for the AuNPs, while no such strong peak was observed with the use of the PtNP matrix, even though the difference of LP is relatively small. No ion from angiotensin I was obtained from AgNPs or CuNPs, even at a high laser fluence of LP100 or more.

As can be seen in the spectra in Fig. 2, Ag and Cu showed no ion peak of angiotensin I when using a higher laser power.

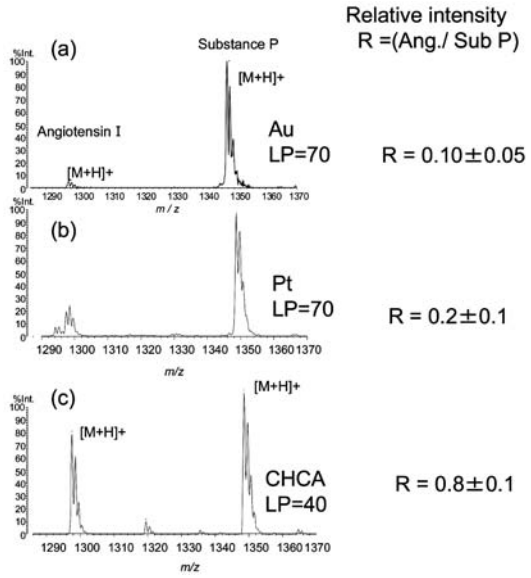

Fig. 3 Mass spectra of mixture of equal concentrations of peptides, angiotensin I (2.5 pmol) and substance P (2.5 pmol) obtained from (a) Au nanoparticles, (b) Pt nanoparticles as SALDI matrixes, as well as (c) α-cyano-4-hydroxycinnamic acid (CHCA) as MALDI matrixes. Substance P is preferentially detected by NPs SALDI-MS. The –S–CH_3 group of methionine (CH_3–S–$(CH_2)_2$–CH(NH_2)–COOH) of substance P has a relatively strong interaction with the gold and platinum nanoparticle surfaces.

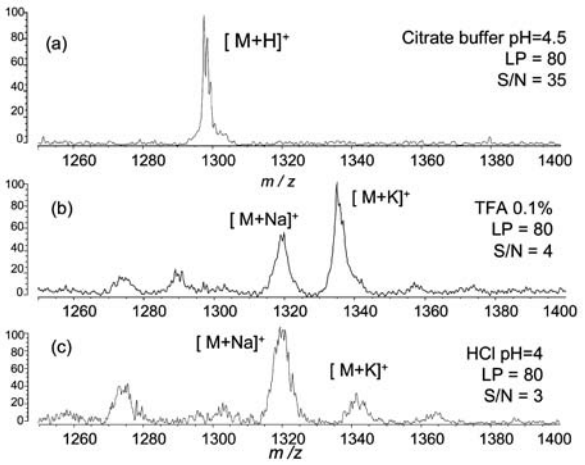

Fig. 4 SALDI-MS spectra of angiotensin I (500 fmol) obtained using Au nanoparticles as a SALDI matrix with various cationization species. (a) Citrate buffer (pH 4.5), (b) 0.1% of trifluoroaceitc acid, (c) HClaq (pH 4).

Thus, it can be concluded that AuNPs and PtNPs are preferable as matrixes for the SALDI-MS of the peptide; AgNPs and CuNPs are not suited for the SALDI-MS of the peptide. In particular, PtNPs have the highest performance for the SALDI-MS of peptides among the NPs studied.

We then subsequently selected AuNPs and PtNPs as SALDI-MS matrixes.

One should be careful about copper nanoparticles, because they may be oxidized after preparation. However, the copper nanoparticles used here were not oxidized in a dispersion, even without a stabilizing reagent, and always showed a red color (CuO is black), and as shown in Fig. 1(a). Even on the substrate, they showed strong plasmon absorption, which is specific for metallic copper nanoparticles. Furthermore, CuO particles can work well as SALDI-MS matrixes.[52] Therefore, it is very reasonable to conclude here that metallic copper nanoparticles are not very suitable for SALDI-MS matrixes.

Selective desorption of peptides

Peptides consist of various amino acids. As described in the above section, the adsorption properties of analyte molecules strongly affect the sensitivity in mass spectrometry. A 1:1 mixture (each 2.5 pmol) of angiotensin I and substance P was deposited on the AuNPs and the PtNPs. As shown in Fig. 3, the peak of substance P is considerably larger than that of angiotensin I in the mass spectra obtained from the SALDI-MS of AuNPs (angiotensin I/substance P (R) = 0.1) and PtNPs (R = 0.2). However, in the MALDI-MS spectrum with CHCA as the organic matrix, the peak of substance P is slightly larger than that of angiotensin I (R = 0.8). The selective desorption and ionization of the adsorbed peptide, substance P, was observed on both nanoparticles. This selective desorption should be attributed to methionine contained in substance P. Sulfur is effectively adsorbed on metal surfaces. Methionine has a –S–CH_3 group that can be effectively coordinated to the surface of metal nanoparticles,[53] resulting in a preferential detection of substance P in a SALDI-MS profile. This result suggests that an efficient rapid heating of metal nanoparticles, themselves, is effective for the soft desorption of peptides from the particle surface.

Cationization species

When using AuNPs and PtNPs as SALDI matrixes, the use of citrate buffer as the proton source was favorable in terms of the intensity and resolution of the mass spectra of the peptides. Figure 4(a) shows the mass spectra of angiotensin I with AuNPs in the presence of citrate buffer at pH 4.5, giving a peak of the proton adduct form of $[M+H]^+$ (m/z = 1298 Da: (a) 150 mV) in the mass spectrum (on the other hand, in Figs. 4(b) and 4(c): (b) Na, 18 mV; K, 35 mV, (c) Na, 4 mV; K, 1.2 mV). However, when trifluoroacetic acids and HCl were used as proton sources, the spectra were much less intense than those obtained using citrate buffer; the peaks in the alkali cation adduct forms of $[M+Na]^+$ (m/z = 1320 Da) and $[M+K]^+$ (m/z = 1336 Da) were of poor quality with lower *S/N* ratios at the same LP value, as shown in Figs. 4(b) and 4(c), respectively. HClaq (pH 4, [HCl] $\approx 10^{-4}$ mol dm^{-3}) should not strongly affect the structure of AuNPs. In the case of the addition of TFA or HCl as cationization species, a small fragment peak at $m/z \approx 1268$ Da could be observed. This fragment may have resulted from the loss of $3H_2O$ or NH_3 and $2H_2O$ or $2NH_3$ and H_2O of the Na adduct of angiotensin I. Comparing these three mass spectra, it can be concluded that ammonium citrate not only donates protons to the analyte molecules, but also chelates alkali cations,[38] which may prevent or greatly minimize their adduction to the analyte. Thus, the addition of a large amount of citrate buffer as an extra proton source was essential for obtaining abundant proton-adducted analyte ions ($[M+H]^+$) of peptides using AuNPs and PtNPs matrixes. Note that citrate buffer is also suitable for the ionization of analytes in titania (TiO_2) matrix systems.[38]

Protective agents of NPs

In general, synthetic approaches for metal nanoparticles have been made using organic protective agents, such as citrate ions, thiols, surfactants, and polymers to aid the stabilization of these particles in aqueous, organic, and thin media.[50,54,55] However, the presence of such protective agents on the nanoparticle

surface might reduce the sensitivity of SALDI-MS.[56-59] As described above, we chose the laser ablation process to obtain metal nanoparticle dispersions because itdoes not always need stabilizing reagents.

In this study, in order to understand the effect of the stabilizing molecules surrounding the nanoparticle surface, we also examined the mass spectra of angiotensin I with sodium citrate ion-protected AuNPs (NaCit-AuNPs) and PVP (poly(*N*-vinyl-2-pyrrolidone))-protected AuNPs and PtNPs (PVP-AuNPs and PVP-PtNPs, respectively) in the presence of citrate buffer at pH 4.5. In contrast to that obtained using metal NPs without protective agents, the mass spectrum obtained using NaCit-AuNPs showed low-quality peaks of the Na^+ and K^+ adduct forms of $[M+Na]^+$ (m/z = 1320 Da) and $[M+K]^+$ (m/z = 1336 Da), and no peaks were observed from the peptide with PVP-PtNPs or PVP-AuNPs, even at a high LP value. Thus, it is evident that the use of unprotected AuNPs and PtNPs is superior to NPs with protective agents such as sodium citrate ions and PVP. The NP matrixes without protective agents, developed in this study have a great advantage in terms of the sensitivity for SALDI-MS, which is an advantage of the laser ablation of nanoparticle production.

Adsorption behavior of various surfactants on nanoparticles

In SALDI-MS using particle suspension matrixes, ions originate predominantly from analyte molecules adsorbed onto the particle surface.[60] In order to examine the adsorption behavior of the cationic surfactants on unprotected AuNPs and PtNPs, we put these nanoparticles into mixed solutions of equal concentrations of the four types of alkyltrimethylammonium surfactants.

These cationic surfactants adsorb onto gold and platinum surfaces from aqueous solutions.[44] Figure S1 shows the mass spectra of equal concentrations of these four cationic surfactants (see Supporting Information, each 1 mM) with the use of AuNP and PtNP matrixes. The cationic surfactants trapped by the isolated particles were characterized by SALDI-MS with AuNPs and PtNPs after simple washing with water. For a comparison, the mass spectra of equal concentrations of these surfactants (each 1 mM) obtained using the chemical matrixes of CHCA, 2,5-dihydroxybenzoic acid (DHBA), and dithranol are also shown in the figure. We observe roughly equal intensities for all surfactants without bromide counterions at m/z values. Even with the CHCA matrix, the peak intensities of the matrix-related ion are very low, which may be a suppression effect of the C16TAB surfactants.[61] When the PtNP or the AuNP matrix is used, on the other hand, the obtained mass spectrum shows the highest ion intensities for cationic surfactants with longer alkyl chains (Figs. S1(a) and S1(b)). C14TAB was observed to be slightly better than C10TAB and C12TAB; C16TAB shows a considerably high peak.

We previously showed that the structures of alkyltrimethyl-ammonium type cationic surfactants on PtNPs differ with the chain length.[62] ^{13}C NMR measurements revealed that surfactant molecules have a *trans* conformation. Diffusion coefficient measurements of CnTAB-stabilized Pt nanoparticles (CnTAB-PtNPs) provided the Stokes' radii of the particles. The Stokes' radii of C10TAB- and C12TAB-PtNPs are much smaller than the sum of the radii of the metal core and the Stokes' radii of the surfactants, themselves. On the other hand, the Stokes' radii of C14TAB- and C16TAB-PtNPs are almost equal to the sum of the radii of the metal core and the Stokes' radii of the surfactants, themselves. This indicates that surfactants with shorter alkyl chains have a tendency to be strongly adsorbed to the particle surfaces at their hydrophobic alkyl chains, while keeping their alkyl chains extended in a *trans* conformation. On the other hand, in the case of surfactants with longer alkyl chains, they may have almost the same structure as free micelles. Another possible reason for this behavior may be that the C16TAB surfactant preferentially adsorbs onto the PtNPs surfaces from the surfactant aqueous solution near to the critical micelle solution concentration (cmc) of 1 mM. Therefore, in the case of C16TAB, the amount of the adsorbed surfactant molecules is higher than that of the other surfactants. These SALDI-MS spectra well correspond to these previous investigation results.

These SALDI-MS results indicate that PtNPs and AuNPs are suitable probes for the selective adsorption of surfactant molecules on nanoparticle surfaces.

Comparison of the performance of various NPs among metals

AuNPs, PtNPs, AgNPs, and CuNPs show distinct differences in performance in the SALDI-MS of peptides. Energy transfer from NPs to analytes likely occurs *via* a thermally driven process, similar to the mechanism proposed by Tanaka *et al*.[27] Thus, one possible explanation for the observed differences is a difference in temperature rise during laser light illumination among these metal nanoparticles, similar to that in the case of particle suspension matrixes in glycerol.[59] Here, the heat diffusion length, d_{diff}, during a laser pulse duration of τ (3 – 11 ns) is given by

$$d_{diff} \approx 2\sqrt{\tau\lambda/\rho C_P}, \quad (1)$$

where λ is the heat conductivity, C_P the heat capacity of the particle material, and ρ the density. For all of the size distributions used in this study, the calculated heat diffusion lengths (d_{diff}) of the nanoparticles used here are much larger than the NP diameter (Table 1) of Ag, Au, Cu, and Pt. Thus, it would be reasonable for the entire NP volume to effectively result in the same temperature, and major differences in NP behavior over the particular size regime (2 – 10 nm) are not a size effect, but different materials.

Assuming that most of the UV laser light is absorbed in the particle surface, the laser-induced temperature increase in the particle surface, ΔT, is[58]

$$\Delta T = \frac{E_p}{\rho V C_P} = \frac{H}{\rho d C_P}, \quad (2)$$

where E_p is the laser pulse energy, H the fluence E_p/A (surface area), and d the diameter of the irradiated area. In this case, ΔT is independent of the particle size. Using constant values for H and d, the $\Delta T(X)/\Delta T(Cu)$ ratios are as follows: 1.38 for X = Au, 1.20 for X = Pt, and 1.39 for X = Ag. The peak temperature of CuNPs is smaller than those of the other NPs. In fact, no Cu cluster ions were observed in the spectra of CuNPs, whereas many Au cluster ions and Ag cluster ions were observed in the spectra of AuNPs and AgNPs, respectively. This is consistent with the difference in the peak temperature. As a result, CuNPs are not suited for the SALDI-MS of peptides and lipids, although they have strong absorbance at a wavelength of 337 nm. Pt cluster ions in the spectra of PtNPs were also relatively few, which may be due to the high melting temperatures of the metals used: 1769°C for bulk Pt, 1064°C for Au, 1083°C for Cu, and 962°C for Ag. Although the use of AuNPs was preferable to AgNPs for the SALDI-MS of peptides, the $\Delta T(X)/\Delta T(Cu)$ ratios of the two NPs values are similar. The lower UV absorbance at 337 nm of AgNPs than of AuNPs, may have decreased $\Delta T(Ag)$.

The above considerations neglect the heat transport between

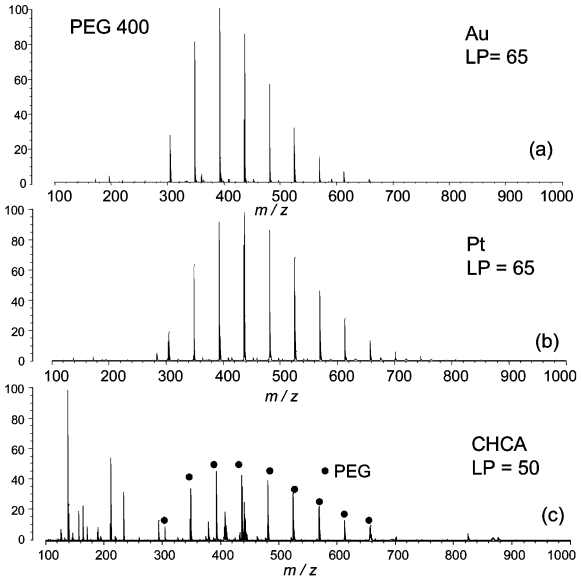

Fig. 5 Mass spectra of polyethyleneglycol, PEG400 (1 mg/mL) obtained using (a) Au nanoparticles, (b) Pt nanoparticles as SALDI matrixes and (c) α-cyano-4-hydroxycinnamic acid (CHCA) as a MALDI organic matrix (circle indicated peaks: from PEG).

particles and the underlying stainless-steel LDI plate. Heat transport decreases the peak temperature of metal nanoparticles during the application of nanosecond laser pulses. The quite low heat conductivity, λ, of PtNPs (Table 1, PtNPs: 71.6, other NPs 317 – 429 W m^{-1} K^{-1}) will have the effect of further increasing ΔT, resulting in the high performance of PtNPs for SALDI-MS.

In order to understand the effect of the heat conductivity as well as the surface area, the SALDI-MS performance of various platinum nanoparticles should be considered. Such experiments are in progress.

Application of NPs to SALDI-MS of synthetic polymers

AuNPs and PtNPs were then applied to the SALDI-MS of synthetic polymers. Figure 5 shows the mass spectra of PEG400 obtained from AuNPs and PtNPs as the SALDI matrixes and from α-cyano-4-hydroxycinnamic acid (CHCA) as the MALDI matrix. AuNPs and PtNPs yielded good spectra with a low noise level in the low-mass range, showing a series of peaks separated at 44 Da intervals that correspond to monomer units of ethylene glycol. As can be seen in Fig. 5(c), when CHCA was used, the spectrum showed many peaks corresponding to the matrix-related ions besides the $[M+Na]^+$ peaks of PEG400. It is clear that the quality of the mass spectra of PEG400 in the low-mass range obtained using the NP matrixes is better than that obtained using the conventional organic matrix of CHCA.

Comparing the three spectra mentioned above, it is clear that the particle size of nanoparticles affects the peak intensities of the mass spectra of synthetic polymers. The peak shapes of the PEG400 mass spectra obtained by PtNP-SALDI and CHCA-MALDI are quite similar. However, in the spectrum obtained by AuNP-SALDI, the peaks of smaller *m/z* are relatively larger than the other two spectra. The peak at *ca.* *m/z* = 390 is the highest in the AuNP-SALDI spectrum.

AuNPs can detect PEG polymers with higher molecular weights (that is, PEG1000, PEG2000, and PEG3000), as shown in Fig. 6. However, although the peaks of the fragmented molecules were not very reproducible, the fragmentation of

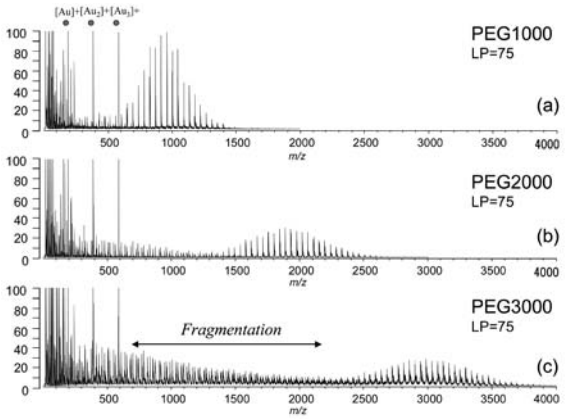

Fig. 6 Mass spectra of (a) PEG1000, (b) PEG2000, and (c) PEG3000 (1 mg/mL) obtained from Au nanoparticles as a SALDI matrix. Peaks according to the Au clusters are observed. Fragmentation of PEG molecules are observed in lower *m/z* regions.

PEGs with increasing molecular weight is dominant for the AuNP matrix than that for the CHCA matrix. On the other hand, in the case of PMMA, no fragmentation was observed, but the peaks at smaller *m/z* were much larger than that for the DHBA matrix, as shown in Fig. 7. This phenomenon supports the discussions on the LDI-MS with particle suspension matrixes reported by Hillenkamp,[60] which noted that the mass analytical sensitivity decreases sizably. The PtNP matrix was also used for SALDI-MS of PEG1000, 2000, and 4000, but the fragmentation of PEGs was observed.

Generally, polymer molecules are adsorbed onto solid surfaces at many points. Therefore, even if the interaction between polymer molecules and the surface is not so strong, polymers do not easily detach from the surface. The high energy of the polymers during the LDI process may be the main reason for fragmentation. It is considered that the strength of the adsorption of the PEG polymer onto the NPs increases with the molecular weight of the adsorbed polymer, owing to the increase in the number of possible binding sites. Their desorptions for the PEG polymer with higher molecular weights would require faster heating and/or higher peak temperatures, resulting in an increase in the degree of excitation of the inner degrees of freedom of the polymers.

Conclusion

In this work, we investigated the mass applications of various noble-metal nanoparticles (*i.e.*, Ag, Au, Cu and Pt) as SALDI-MS matrixes for peptides and synthetic polymers, to examine the effect of the nanoparticle species on metal elements. It is concluded that the use of AuNPs and PtNPs as matrixes is preferable over AgNPs and CuNPs for the SALDI-MS of peptides. The quality of the mass spectra obtained using the PtNP matrix is better than that obtained using the AuNP matrix. The addition of a large amount of citrate buffer as an extra proton source is essential for obtaining better-quality results of the mass analysis of peptides using metal nanoparticle matrixes. The use of unprotected AuNPs and PtNPs is superior to that of NPs with protective agents, such as sodium citrate ions and PVP. These results indicate that PtNPs and AuNPs are suitable probes for the selective desorption of species adsorbed onto the nanoparticle surfaces. The selectivity of the adsorbed surfactants on nanoparticles is better with the PtNP matrix than

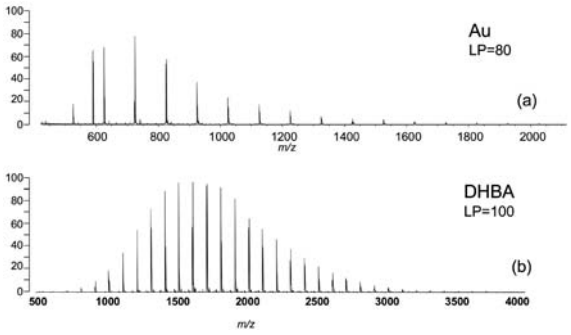

Fig. 7 Mass spectra of PMMA (1 mg/mL) obtained from (a) Au nanoparticles as a SALDI matrix and (b) DHB as a MALDI organic matrix.

with the AuNP matrix; the selective desorption of adsorbed surfactants on nanoparticles is possible with the use of the PtNP matrix, even with excess surfactants. The high performance of PtNPs can be explained by the lower heat conductivity of Pt.

Acknowledgements

This work was financially supported in part by Grants-in-Aid for Scientific Research (Nos. 17655059, 19350045) and Grants-in-Aid for Scientific Research in Priority Areas (Strong Photon-Molecule Coupling Fields for Chemical Reactions (470, No. 20043011), and Molecular Science for Supra Functional Systems (477, No. 20050007)) from the Ministry of Education, Culture, Sports, Science and Technology (MEXT), Japan. The partial financial support to T. Y. from Collaboration of Regional Entities for the Advancement of Technological Excellence (CREATE) organized by HYOGO Prefecture funded by Japan Science and Technology Agency (JST) is also gratefully acknowledged. T. Y. thanks Prof. H. Nishihara (Univ. Tokyo) for his warm hospitality for his assistance to the completion of this work.

Supporting Information

Variation of the cationic surfactants and their SALDI-MS spectra are collected in the supporting information. This material is available free of charge on the Web at http://www.jsac.or.jp/analsci/.

References

1. G. Schmid, *Chem. Rev.*, **2002**, *102*, 1709.
2. M. A. El-Sayed, *Acc. Chem. Res.*, **2001**, *34*, 257.
3. M.-C. Daniel and D. Astruc, *Chem. Rev.*, **2004**, *104*, 293.
4. N. Toshima and T. Yonezawa, *New J. Chem.*, **1998**, *22*, 1179.
5. A. P. Alivisatos, *J. Phys. Chem.*, **1996**, *100*, 13226.
6. M.-P. Pileni, *Nat. Mater.*, **2003**, *2*, 145.
7. P. Buffat and J. P. Borel, *Phys. Rev. A*, **1976**, *13*, 2287.
8. R. Jin, Y. Cao, C. A. Mirkin, K. L. Kelly, G. C. Schatz, and J. G. Zheng, *Science*, **2001**, *294*, 1901.
9. J. Aizpura, P. Hanarp, D. S. Sutherland, M. Käll, G. W. Bryant, and F. J. García de Abajo, *Phys. Rev. Lett.*, **2003**, *90*, 057401.
10. M. Moreno-Mañas and R. Pleixats, *Acc. Chem. Res.*, **2003**, *36*, 638.
11. C. A. Mirkin, R. L. Letsinger, R. C. Mucic, and J. Storhoff, *Nature*, **1996**, *382*, 607.
12. M. Han, X. Gao, J. Z. Su, and S. Nie, *Nat. Biotechnol.*, **2001**, *19*, 631.
13. S. Sun, C. B. Murray, D. Weller, L. Folks, and A. Moster, *Science*, **2000**, *287*, 1989.
14. P. V. Kamat, *J. Phys. Chem. B*, **2002**, *106*, 7729.
15. D. A. Schultz, *Curr. Opin. Biotechnol.*, **2003**, *14*, 13.
16. R. Elghanian, J. J. Storhoff, R. C. Mucic, R. L. Letsinger, and C. A. Mirkin, *Science*, **1997**, *277*, 1078.
17. J. Jiang, K. Bosnick, M. Maillard, and L. Brus, *J. Phys. Chem. B*, **2003**, *107*, 9964.
18. S. Nie and S. R. Emory, *Science*, **1997**, *275*, 1102.
19. M. Moskovits, *Rev. Mod. Phys.*, **1985**, *57*, 783.
20. T. Yonezawa and N. Toshima, *J. Mol. Catal.*, **1993**, *83*, 167.
21. N. K. Chaki, H. Tsunoyama, Y. Negishi, H. Sakurai, and T. Tsukuda, *J. Phys. Chem. C*, **2007**, *111*, 4885.
22. R. M. Crooks, M. Zhao, L. Sun, V. Chechik, and L. K. Yeung, *Acc. Chem. Res.*, **2001**, *34*, 181.
23. G. C. Bond, *Catal. Rev.—Sci. Eng.*, **1999**, *41*, 319.
24. M. Haruta, *Catal. Today*, **1997**, *36*, 153.
25. N. Lopez and J. K. Norskov, *J. Am. Chem. Soc.*, **2002**, *124*, 11262.
26. M. Karas and F. Hillenkamp, *Anal. Chem.*, **1988**, *60*, 2299.
27. K. Tanaka, H. Waki, Y. Ido, S. Akita, Y. Yoshida, and T. Yoshida, *Rapid Commun. Mass Spectrom.*, **1988**, *2*, 151.
28. K. Dreisewerd, *Chem. Rev.*, **2003**, *103*, 395.
29. G. Montaudo, F. Samperi, and M. S. Montaudo, *Prog. Polym. Sci.*, **2006**, *31*, 277.
30. J. Schiller, R. Suss, J. Arnhold, B. Fuchs, J. Lessig, M. Muller, M. Petkovic, H. Spalteholz, O. Zschoring, and K. Arnold, *Prog. Lipid. Res.*, **2004**, *43*, 449.
31. R. Balasubramanian, R. Guo, A. J. Mills, and R. W. Murray, *J. Am. Chem. Soc.*, **2005**, *127*, 8126.
32. H. Kawasaki, T. Yonezawa, T. Watanabe, and R. Arakawa, *J. Phys. Chem. C*, **2007**, *111*, 16278.
33. M. V. Ugarov, T. Egan, D. V. Khabashesku, J. A. Shultz, H. Peng, V. N. Khabashesku, H. Furutani, K. S. Prather, H.-W. J. Wang, S. N. Jacknson, and A. S. Woods, *Anal. Chem.*, **2004**, *76*, 6734.
34. J. Wei, J. M. Buriak, and G. Siuzdak, *Nature*, **1999**, *399*, 243.
35. S. A. Trauger, E. P. Go, Z. Shen, J. V. Apon, B. J. Compton, E. S. P. Bouvier, M. G. Finn, and G. Siuzdak, *Anal. Chem.*, **2004**, *76*, 4484.
36. S. Okuno, R. Arakawa, K. Okamoto, Y. Matsui, S. Seki, T. Kozawa, S. Tagawa, and Y. Wada, *Anal. Chem.*, **2005**, *77*, 5364.
37. C.-T. Chen and Y.-C. Chen, *Anal. Chem.*, **2004**, *76*, 1453.
38. C.-T. Chen and Y.-C. Chen, *Rapid Commun. Mass Spectrom.*, **2004**, *18*, 1956.
39. X. Wen, S. Dagan, and V. H. Wysocki, *Anal. Chem.*, **2007**, *79*, 434.
40. C.-H. Teng, K.-C. Ho, Y.-S. Lin, and Y.-C. Chen, *Anal. Chem.*, **2004**, *76*, 4337.
41. Y.-F. Huang and H.-T. Chang, *Anal. Chem.*, **2006**, *78*, 1485.
42. J. S. Kirk and P. W. Bohn, *J. Am. Chem. Soc.* **2004**, *126*, 5920.
43. J. A. McLean, A. A. Stumpo, and D. H. Russell, *J. Am. Chem. Soc.*, **2005**, *127*, 5305.
44. H. Kawasaki, K. Nishimura, and R. Arakawa, *J. Phys. Chem. C*, **2007**, *111*, 2683.
45. J. Sunner, E. Dratz, and Y.-C. Chen, *Anal. Chem.*, **1995**, *67*,

4335.
46. S. Zumbuhl, R. Knochenmuss, S. Wulfert, F. Dubois, M. J. Dale, and R. A. Zenobi, *Anal. Chem.*, **1998**, *70*, 707.
47. H. Zhang, S. Cha, and E. S. Yeung, *Anal. Chem.*, **2007**, *79*, 6575.
48. F. Mafuné, J. Kohno, Y. Takeda, T. Kondow, and H. Sawabe, *J. Phys. Chem. B*, **2000**, *104*, 9111.
49. F. Mafuné, J. Kohno, Y. Takeda, T. Kondow, and H. Sawabe, *J. Phys. Chem. B*, **2001**, *105*, 5114.
50. G. Frens, *Nat. Phys. Sci.*, **1973**, *241*, 20.
51. H. Kawasaki, T. Sugitani, T. Watanabe, T. Yonezawa, H. Moriwaki, and R. Arakawa, *Anal. Chem.*, **2008**, *80*, 7524.
52. T. Yonezawa, H. Kawasaki, K. Sato, H. Nishihara, and R. Arakawa, *Polym. Prepr. Jpn.*, **2008**, *57*, 917.
53. T. Kinoshita, S. Seino, Y. Mizukoshi, Y. Otome, T. Nakagawa, K. Okitsu, and T. A. Yamamoto, *J. Magn. Magn. Mater.*, **2005**, *293*, 106.
54. N. Toshima, K. Kushihashi, T. Yonezawa, and H. Hirai, *Chem. Lett.*, **1989**, 1769.
55. M. Brust and C. J. Kiely, *Colloids Surf., A*, **2002**, *202*, 175.
56. S. L. Cohen and B. T. Chait, *Anal. Chem.*, **1996**, *68*, 31.
57. J. Yao, J. R. Scott, M. K. Young, and C. L. Wilkins, *J. Am. Soc. Mass Spectrom.*, **1998**, *9*, 805.
58. I. D. Figueroa, O. Torers, and D. H. Russell, *Anal. Chem.*, **1998**, *70*, 4527.
59. C.-L. Su and W.-L. Tseng, *Anal. Chem.*, **2007**, *79*, 1626.
60. M. Schurenberg, K. Dreisewerd, and F. Hillenkamp, *Anal. Chem.*, **1999**, *71*, 221.
61. Z. Guo, Q. Zhang, H. Zou, B. Guo, and J. Ni, *Anal. Chem.*, **2002**, *74*, 1637.
62. T. Yonezawa, N. Toshima, C. Wakai, M. Nakahara, M. Nishinaka, T. Tominaga, and H. Nomura, *Colloids Surf., A*, **2000**, *169*, 35.
63. "*CRC Handbook of Chemistry and Physics*", 88th ed., **2007**, CRC Press, 12 – 200.